Laboratory Evaluation of the gForce Tracker^{TM}, a Head Impact Kinematic Measuring Device for Use in Football Helmets

KODY R. CAMPBELL ,[1,4] MEAGAN J. WARNICA,[2] IRIS C. LEVINE,[2] JEFFREY S. BROOKS,[1] ANDREW C. LAING,[2] TIMOTHY A. BURKHART,[3] and JAMES P. DICKEY[1]

[1]Joint Biomechanics Lab, School of Kinesiology, Western University, Thames Hall, 1151 Richmond St., London, ON N6A 3K7, Canada; [2]Injury Biomechanics and Aging Laboratory, Department of Kinesiology, University of Waterloo, 200 University Ave West, Waterloo, ON N2L 3G1, Canada; [3]Mechanical and Materials Engineering, Thompson Engineering Building, Western University, 1151 Richmond St., London, ON N6A 5B9, Canada; and [4]Department of Allied Health Sciences, The University of North Carolina at Chapel Hill, 2207 Stallings-Evans Sports Medicine Center, Campus Box 8700, Chapel Hill, NC 27599, USA

Abstract—This study sought to compare a new head impact-monitoring device, which is not limited to specific helmet styles, against reference accelerometer measurements. Laboratory controlled impacts were delivered using a linear pneumatic impactor to a Hybrid III headform (HIII) fitted with a football helmet and the impact monitoring device (gForce Tracker-GFT) affixed to the inside of the helmet. Linear regression analyses and absolute mean percent error (MAPE) were used to compare the head impact kinematics measured by the GFT to a reference accelerometer located at the HIII's center of mass. The coefficients of determination were strong for the peak linear acceleration, peak rotational velocity, and HIC$_{15}$ across all impact testing locations ($r^2 = 0.82$, 0.94, and 0.70, respectively), but there were large MAPE for the peak linear acceleration and HIC$_{15}$ (MAPE = 49 ± 21% and 108 ± 58%). The raw GFT was accurate at measuring the peak rotational velocity at the center of mass of the HIII (MAPE = 9%). Results from the impact testing were used to develop a correction algorithm. The coefficients of determination for all impact parameters improved using the correction algorithm for the GFT ($r^2 > 0.97$), and the MAPE were less than 14%. The GFT appears to be a suitable impact-monitoring device that is not limited to specific styles of football helmets, however, correction algorithms will need to be developed for each helmet style.

Keywords—Concussion, mTBI, Head acceleration, Head impact biomechanics, Impact monitoring, Helmet sensors.

INTRODUCTION

Every year, as many as 3.6 million individuals suffer a sport- or recreation-related traumatic brain injury, of which the vast majority involve youth and adolescents.[12] The incidence rates for mild traumatic brain injury, or concussion, vary by sport. For male athletes in the United States, football consistently has a high incidence of concussion, more than 6.4 concussions per 10,000 athletic exposures.[14] Failure to properly diagnose and manage concussion can have catastrophic consequences, particularly in cases of severe brain injury or death after a second injury is sustained before symptoms from the initial injury are fully resolved.[24] Athletes commonly fail to report symptoms during activity, which further complicates the clinical management of concussion.[16] To our knowledge, no studies have investigated the long-term effects of youth and/or high school participation in contact sports, however, recent studies on professional football players showed that multiple concussions can lead to detrimental long-term effects on brain function, along with early onset of Alzheimer's Disease and depression.[9,10] Additionally, there is a growing concern that sub-injurious or "sub-concussive" head impacts that do not result in a diagnosed or identifiable brain injury at the time of impact lead to the neurological issues seen in retired athletes. Recent research involving high school football players suggests that there may be a cumulative (season-long) effect of sub-concussive impacts on the brain's white matter connectivity.[15] The mechanisms of injury for sport concussion and sub-concussive impacts are related to excessive linear and

Address correspondence to Kody R. Campbell, Department of Allied Health Sciences, The University of North Carolina at Chapel Hill, 2207 Stallings-Evans Sports Medicine Center, Campus Box 8700, Chapel Hill, NC 27599, USA. Electronic mail: kcampb@live.unc.edu

rotational accelerations of the head resulting from head impacts.[8,27]

The standard Head Impact Telemetry (HIT) System offers a real-time biomechanical assessment of the linear and rotational head accelerations experienced by football players as they compete in games and practices, and has been used extensively in the last decade to capture over 1.2 million impacts.[23] The standard HIT System encoder, however, can only be used with three styles of football helmets, limiting its capabilities to collect data from different manufacturers' helmets. Additionally, the orientation of the accelerometers in a standard HIT system encoder calculates the peak resultant rotational acceleration of impacts, and does not calculate rotational accelerations in the transverse plane. Importantly, computer simulations, using the SIMon finite element model, showed that head accelerations in the transverse plane caused 0.55–1.7 times more cumulative strain on brain tissue than head accelerations without rotations in the transverse plane.[26,29] This is a limitation of the standard HIT system. However, since the development of the standard HIT system an enhanced version of the HIT system has been developed that uses 12 accelerometers and provides 6 degree of freedom (6DOF) linear and rotational head accelerations.[21] Additionally, a hockey version and a soccer version of the HIT system provide 6DOF linear and rotational head accelerations.[11,17] These advanced versions of the HIT system calculate rotational accelerations based on the output of linear accelerometers rather than directly measuring the rotational acceleration of head impacts. Other companies have also developed alternative devices to record the magnitude and frequency of head impacts. Importantly, these devices are not limited to specific football helmets, can be affixed to many styles of helmets from different helmeted sports, and use gyroscopes to directly measure rotational kinematics of the head.

A Canadian company, Artaflex Inc. (Markham, Ontario, Canada), has developed a head impact kinematic measurement system, the gForce Tracker (GFT), for measuring 6DOF head kinematics sustained from impacts. The GFT device can be coupled to the inside of the helmets of football players and outputs real-time results of the linear acceleration, rotational velocity, impact location, and severity (Head Impact Criterion; HIC_{15}) of each helmet impact.[28] One limitation of the GFT is that it does not calculate the rotational acceleration of head impacts, which relate to axonal injury in the brain,[27] but this impact parameter can be calculated by differentiating the rotational velocity data. The GFT device was recently evaluated for use in hockey helmets.[1] That study showed moderate associations, $r^2 > 0.60$, for linear acceleration, and strong associations for rotational velocity, $r^2 > 0.83$, between the GFT and the gold standard reference accelerometer fixed inside a Hybrid III headform (HIII) anthropometric test device during controlled laboratory impacts. However, the authors concluded that the mounting location of the GFT and the style of helmet affect the accuracy of the device's measurements. Thus, before this device can be implemented into football helmets, the accuracy of the device's head impact kinematics needs to be quantified. Therefore, the purpose of this study was to compare the GFT's estimates of peak linear acceleration, peak rotational velocity, and HIC_{15} with measurements from a reference accelerometer package at the center of mass (CM) of a HIII headform during controlled laboratory impacts. Results of the comparison between the GFT and the HIII were used to develop algorithms to predict the impact parameters at the CM of the HIII from head impact kinematics measured by the GFT.

METHODS AND MATERIALS

Testing Apparatus

Impacts were delivered to a 50th percentile Hybrid III headform and neck (Humanetics, Plymouth, MI) fitted with a medium sized Riddell Revolution Speed Helmet (Riddell, Elyria, OH) using a linear pneumatic impactor (Biokinetics Inc., Ottawa, Canada; Fig. 1), similarly to other researchers.[2,19,21] When triggered, a solenoid dump valve released pressurized air to a pneumatic actuator that accelerated a 14.3 kg impacting ram toward the headform system. At the time of impact with the helmet, the impacting ram was detached from the actuator to ensure that it was not actively being driven into the headform system. The impactor face was made up of an ultra-high molecular weight polyethylene plate with the same curvature as the tested helmet. To better represent helmet-to-helmet contact, a 35 mm layer of vinyl nitrile foam (VN600, DerTex, Saco, Maine) was placed behind the polyethylene plate.[3,20,22] A light-gate sensor was used to measure the velocity of the impacting ram, as well as trigger the data collection system.

The masses of the HIII head and neck were 4.54 and 1.54 kg, respectively, and a cable within the neck was tensioned to produce a neck stiffness of 1.1 Nm per manufacturer's standards. A nylon stocking covered the headform to reduce friction while fitting the helmet, and to better simulate the friction of a real human head during the impacts.[2,21] The head and neck were fastened to a low friction sliding table, which allowed the system to translate in the direction that it was being impacted. The sliding table enabled different impact
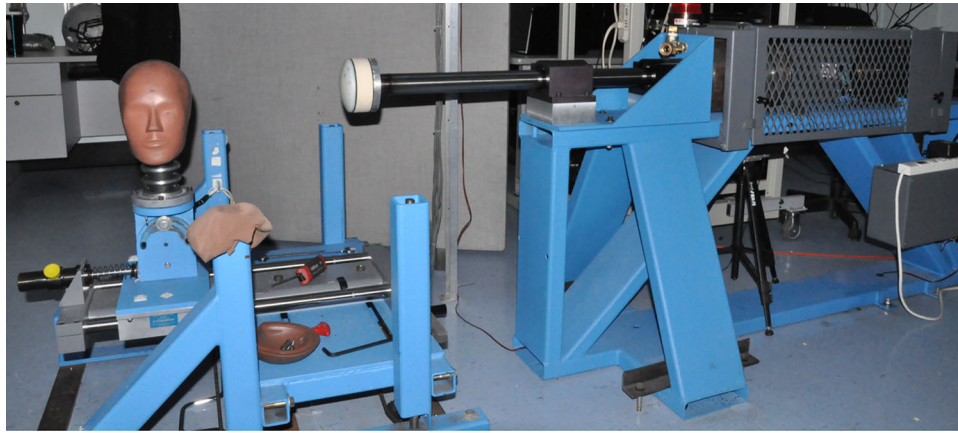
FIGURE 1. Pneumatic linear impactor with HIII headform and neck attached to sliding table.

FIGURE 2. Location of the GFT inside the helmet.

locations by adjusting the height in the *z*-axis (superior/inferior) as well as adjusting the position in the *y*-axis (medial/lateral). Two additional attachments rotated the head about the *z*-axis (yaw) and *y*-axis (pitch) to achieve the desired impact locations, which will be described in the testing protocol section.

The helmet was fit to the HIII according to the helmet manufacturer's specifications. A custom-built aligning tool was used to align the mid-sagittal planes of the HIII and helmet, and to ensure that the top of the helmet opening was 5.08 cm above the brow of the HIII before each trial. The helmet had a standard inflatable liner, and 3.81 cm inflatable jaw pieces. A hand held air pump inflated the padding to approximately 4.5 psi and to achieve a snug fit. An S2BD-LW-V style facemask (Riddell, Elyria, OH) was included as part of the tested system. After every trial the helmet was inspected to ensure that the chinstrap had not moved, no hardware had come loose, and that no part of the system was damaged.

Laboratory Instrumentation and Data Collection

Nine single-axis accelerometers (model 7264B-2000, Endevco Corp., San Juan Capistrano, CA) were arranged in a 3-2-2-2 nine accelerometer package (NAP) orthogonal arrangement at the CM of the HIII and served as the reference accelerometer package.[7] Voltages from the accelerometers were amplified and scaled to a 250 g max (model 136, Endevco Corp., San Juan Capistrano, CA) and passed through an on-board CFC1000 low pass anti-aliasing filter. Signals were digitized using a 16-bit NI 9215 analog-to-digital board module in a NI-cDAQ-9188 system, and were recorded by a custom LabVIEW program (v2010, National Instruments Corp., Austin, TX). When triggered by the light gate, acceleration signals were sampled at 10 kHz for 100 ms. Resultant linear acceleration was calculated from the NAP method using the CFC1000 filtered accelerometer data.[7] Each of the 9-accelerometer signals were further processed with a CFC180 digital filter post collection, in accordance with SAE specifications, to calculate the resultant rotational acceleration from the NAP method.[7,30] Rotational velocities were determined by integrating the rotational acceleration signal and the resultant linear acceleration was used to determine the HIC_{15} injury metric.[28]

Helmet Instrumentation and GFT

The helmet was instrumented with one gForce Tracker (Hardware version: GFT3.s.19, Artaflex Inc., Markham, ON, Canada) that was adhered to the inside of the helmet shell, left of the crown air bladder, using an industrial strength re-closeable fastener (3 M[TM] Dual Lock[TM] Re-closeable Fastener SJ3551 400 Black, 3 M Global Headquarters, St. Paul, MN; Fig. 2).
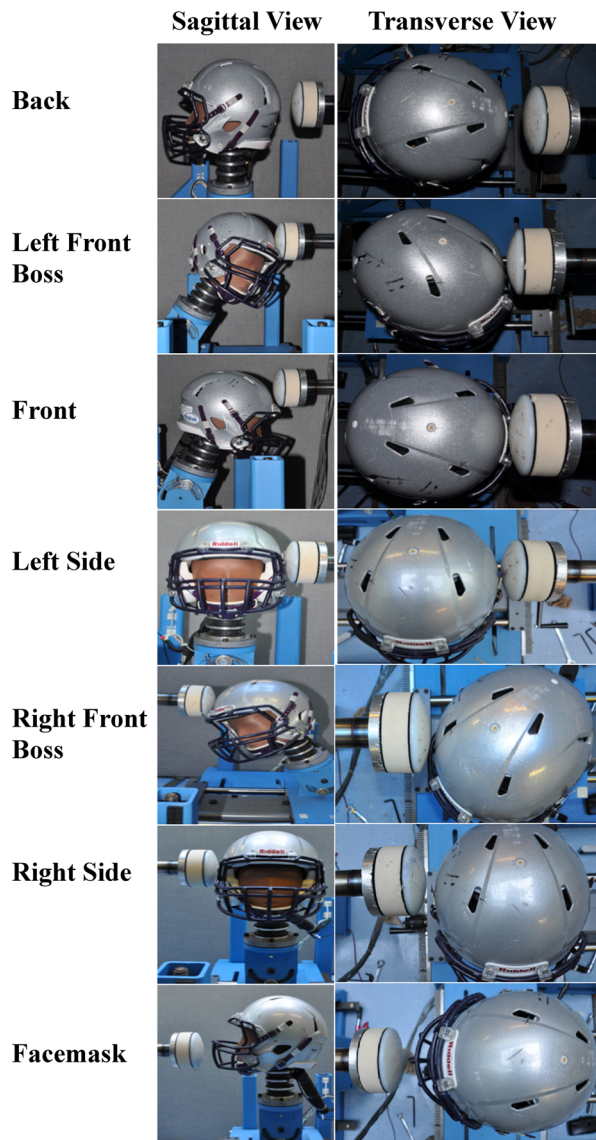
FIGURE 3. Impact testing locations (sagittal and transverse views) for the testing protocol.

The GFT3 measures 50 mm long, 29 mm wide, and 14 mm high, and weighs 2 g. It contains a tri-axial linear accelerometer, a tri-axial gyroscope, as well as a lithium ion rechargeable battery, and on-board memory for storing up to 400 impacts. Each axis of the tri-axial accelerometer had a range of ±200 g and a 1 g resolution. Each axis of the tri-axial gyroscope measured rotational velocity in degrees per second (°/s) and had a range of ±2000°/s. Data were collected when the linear acceleration on any axis was greater than a user-selected threshold; for the purposes of this study the data collection trigger threshold was set to 10 g. To ensure that the entire impact was collected, the device recorded 8 ms of data preceding the threshold, and 32 ms of impact data following the

threshold. Linear acceleration signals were low pass filtered with a 300 Hz anti-aliasing filter and sampled at 3000 Hz. Rotational velocity signals were low pass filtered with a 100 Hz anti-aliasing filter and sampled at 800 Hz. Data were time stamped and recorded to on-board memory.

After all trials for one impact location were completed, and without removing the helmet, the GFT was connected to a laptop by a micro USB cord and the impact data were uploaded to the GFT's Internet software (gManager 1.8) for further processing (see below). Resultant linear accelerations and rotational velocities were calculated for each impact. Peak resultant linear accelerations and rotational velocities were also recorded along with HIC_{15} severity for each trial. The GFT software calculated impact locations with azimuth and elevation coordinates. The 0° azimuth angle was oriented out of the nose and increased up to 359° in a clockwise manner moving from the nose towards the right ear. The 0° elevation angle originated at the level of the Frankfurt plane. Positive elevation angles were between the Frankfurt plane and the top of the head. Negative elevation angles were between the Frankfurt plane and the spine of the neck. The software used the azimuth and elevation coordinates to categorize the location of the impact as quadrants (front, back, right, left, top, or bottom). Azimuth angles between 315° and 45° were categorized as front impacts, while azimuth angles between 135° and 225° were categorized as back impacts. Azimuth angles between 45° and 135° and between 205° and 315° were categorized as right and left side impacts. Lastly, impacts were categorized as top if the elevation angles were greater than 45° and classified as bottom if their elevation angles were less than 45°; this overrode the category that was defined based on the azimuth angle. The impact data were exported to Microsoft Excel 2010 (Microsoft, Redmond, WA) for further interpretation.

Impact Locations and Testing Protocol

Seven locations on the helmet were chosen for the impact testing: back, facemask, front, left front boss, left side, right front boss, and right side (Fig. 3). These locations encompass the majority of the helmet and reflect some locations used in the certification of helmets by the National Operating Committee on Standards for Athletic Equipment (NOCSAE).[18] Impacts at each of these locations were collected at 4 impact velocities specified for the certification of helmets by NOCSAE (3.0, 3.7, 4.2 and 5.5 m/s),[18] as well as 7.0 m/s. Additionally, the six helmet shell locations were tested at 8.5 m/s. These impact velocities represent impacts associated with concussions in National
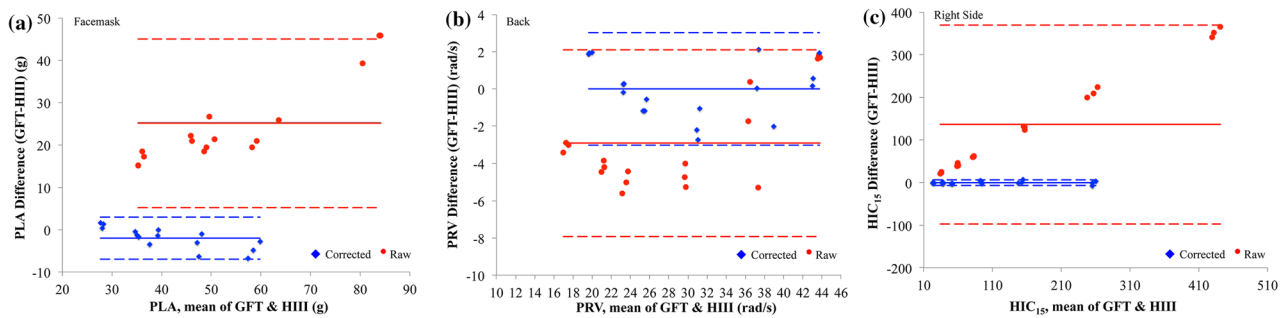
FIGURE 4. Bland-Altman plots for the peak linear acceleration for impacts to the facemask (a), the peak rotational velocity for impacts to the back (b), and HIC_{15} for impacts to the right side (c). These impact locations represented the largest disagreement (largest mean difference and standard deviation of the differences) between the raw GFT and the HIII. Solid red lines represent the mean difference between the raw GFT and the HIII and the red dashed lines represent the 95% intervals around that mean difference. Solid blue lines represent the mean difference between the corrected GFT and the HIII and the blue dashed lines represent the 95% intervals around that mean difference. Using the correction algorithm decreased the mean difference (mean difference closer to zero), and the standard deviations of the differences.

Football League players.[20] The facemask impacts were not performed at the highest velocity, 8.5 m/s, to prevent damage to the helmet. Testing of each impact location was performed in blocks and the order of presentation of each of the impact location blocks was randomized, with the exception of the facemask, which was tested last. For each location, impact velocities were performed in ascending order. A total of 3 trials were performed at each combination of impact velocity and location, for a total of 123 impacts. Sufficient time was allowed after each impact (4 min $\pm$ 15 s) for the protective foam inside the helmet to return to its initial state between trials.

Correction Algorithm

Since the GFT measured the accelerations of the helmet shell, and we were interested in the impact parameter measurements at the CM of the head (peak linear acceleration, peak rotational velocity, and HIC_{15}), we developed a correction algorithm for predicting these parameters that is similar to other researchers.[1] This was important because helmet shell accelerations are larger than the head CM acceleration.[13] Preprocessing for the correction algorithm involved calculating the impact direction based on the azimuth angle calculated by the GFT. The impacts were categorized as front (azimuth angles between 315° and 45°), right side (45°–135°), left side (225°–315°) or back (135°–225°). The version of GFT software used during the testing did not accurately account for the angle of elevation of the GFT within the helmet. Therefore, the angle of elevation was not used to categorize impacts for the correction algorithm. Preprocessing also included filtering the *x*-, *y*-, *z*-axis linear acceleration data from the GFT with a CFC 180 filter, calculating the resultant and extracting the peak

value.[5] The resultant rotational accelerations were calculated by numerically differentiating the resultant raw rotational velocity data from the GFT with respect to time using a 5-point stencil method,[5] and extracting the peak values. Individual correction equations were developed for each of the impact parameters. Each correction equation had a similar structure involving linear combinations of the preprocessed peak resultant linear acceleration, the peak resultant rotational velocity from the GFT, and the peak resultant rotational acceleration. The coefficients for the linear combinations were optimized by minimizing the sum of the squared differences between the parameters measured from the HIII and the GFT.

Data Analysis

Bland–Altman plots were used to evaluate the amount of measurement agreement for the peak linear acceleration, peak rotational velocity, and HIC_{15} magnitudes (our impact parameters) between the HIII and the outputs by the raw GFT (raw GFT).[3] We also evaluated the measurement agreement between the HIII and outputs from the GFT measurements using the correction algorithm (corrected GFT). The *x*, *y* coordinate of the plot represented the amount of measurement agreement between the HIII and the raw GFT. The *x*-coordinate was created by calculating the mean of the impact value measured by the HIII and the raw GFT for a given impact. The difference between the raw GFT and HIII created the *y*-coordinate for the plot. The mean difference of the measurements were calculated and plotted as horizontal line. The 95% limits of agreement provided an interval where 95% of the difference between the measurements by the HIII and raw GFT were expected to lie. The lower and upper limits were estimated by the mean

difference ± the standard deviation of the differences. The same procedure was used for the amount of measurement agreement between the HIII and the corrected GFT. Plots were created for each impact parameter at each impact location. The weakest agreement between the HIII and the raw GFT for an impact location for each impact parameter is presented in the manuscript. Accordingly, the amount of measurement agreement between the HIII and the raw GFT was stronger for the other locations. The corresponding plot between HIII and corrected GFT was presented to evaluate the effect of the correction algorithm. The weakest agreement at a location was chosen based on the largest mean difference from zero, and the largest standard deviation. The full set of plots is presented in supplementary documents.

Linear regression analyses were performed, in Microsoft Excel 2010, on our impact parameters between the HIII, the outputs by the raw GFT, and between the HIII and the corrected GFT. Analyses were performed on all trials ($n = 123$) and stratified by impact site (back, facemask, front, left front boss, left side, right front boss and right side). The regression analysis used the Eq. (1)

$$Y = \beta_0 + \beta_1 X \qquad (1)$$

where Y was the measurement made by the raw GFT or corrected GFT, X was the measurement made by the HIII, β_1 was the slope of the relationship between the raw GFT or corrected GFT and HIII, and β_0 was the offset bias. Ideally, β_1 would be equal to one meaning that there is a one to one relationship between the measurement made by the HIII and the GFT. The coefficient of determination (r^2) was calculated as a measure of goodness of fit for each linear regression model. The same approach was used to evaluate the peak rotational acceleration calculated by the algorithm against the HIII.

Similar to a study that evaluated the GFT in hockey helmets,[1] the absolute percent errors were calculated between the GFT (raw and corrected) measurements of the impact parameters and the HIII to provide an additional indicator of the GFT's accuracy. Absolute percent error was calculated with Eq. (2)

$$\text{Absolute Percent Error} \\ = \frac{|\text{GFT}_{\text{raw or corrected}} - \text{HIII}|}{\text{HIII}} \times 100 \qquad (2)$$

where the $GFT_{\text{raw or corrected}}$ was the impact parameter determined by either the raw GFT or the corrected GFT, and *HIII* was the impact parameter determined from the reference accelerometer package at the CM of the HIII. Mean absolute percent error (MAPE) was calculated for each impact location and across all impacts for each impact parameter. This approach was also used to compare the accuracy of the peak rotational acceleration calculated by the algorithm to the peak rotational acceleration measured by the HIII. A MAPE less than or equal to 10% was chosen as an acceptable amount of error a priori, and coincided with previous research.[1,21]

RESULTS

All trials ($n = 123$) were used to develop the location dependent correction equations for our impact parameters. The back, left side and right side locations each had 18 observations to construct the correction equation. The front location used 69 observations to construct the correction equation. The correction equations, including the coefficients and offsets, are presented in supplementary documents.

The weakest measurement agreement between the HIII and the raw GFT for the peak linear acceleration was at the facemask impact location (Fig. 4a). The
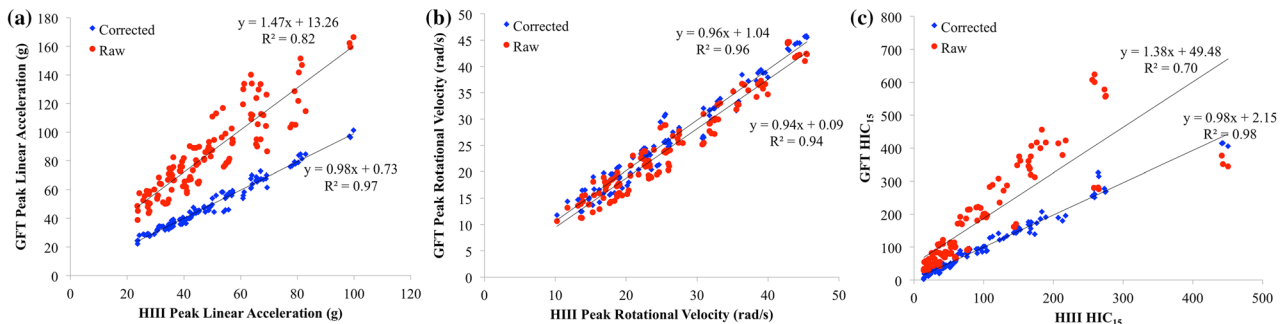
FIGURE 5. Linear regression analyses between the raw GFT (red), and corrected GFT (blue), compared to the HIII for the peak linear acceleration (a), the peak rotational velocity (b), and the HIC₁₅ (c). Measures of association and accuracy of the raw GFT compared to the HIII improved by using the correction algorithm for the peak linear acceleration.

TABLE 1. Mean absolute percent error (MAPE) of the peak linear acceleration, peak rotational velocity, and HIC$_{15}$ between the HIII, raw GFT (rGFT) and corrected GFT (cGFT).

Impact site	Peak linear acceleration		Peak rotational velocity		HIC$_{15}$	
	rGFT	cGFT	rGFT	cGFT	rGFT	cGFT
Back	26 ($\pm$8)	2 ($\pm$1)	13 ($\pm$6)	4 ($\pm$4)	16 ($\pm$6)	13 ($\pm$14)
Facemask	59 ($\pm$12)	5 ($\pm$4)	7 ($\pm$3)	6 ($\pm$3)	99 ($\pm$41)	17 ($\pm$10)
Front	51 ($\pm$18)	8 ($\pm$5)	10 ($\pm$5)	13 ($\pm$7)	105 ($\pm$19)	23 ($\pm$21)
Left front boss	69 ($\pm$9)	8 ($\pm$4)	16 ($\pm$7)	11 ($\pm$4)	189 ($\pm$43)	24 ($\pm$12)
Left side	31 ($\pm$9)	3 ($\pm$2)	7 ($\pm$1)	1 ($\pm$1)	85 ($\pm$22)	5 ($\pm$3)
Right front boss	72 ($\pm$16)	3 ($\pm$3)	2 ($\pm$3)	6 ($\pm$5)	141 ($\pm$37)	15 ($\pm$9)
Right side	39 ($\pm$7)	2 ($\pm$1)	7 ($\pm$2)	1 ($\pm$1)	123 ($\pm$19)	3 ($\pm$2)
All	49 ($\pm$21)	4 ($\pm$4)	9 ($\pm$6)	6 ($\pm$6)	108 ($\pm$58)	14 ($\pm$14)

Values are presented as percent's. In general, the correction algorithm decreased the MAPE for the peak linear acceleration and HIC$_{15}$ across all impact locations.

weakest agreement for the peak rotational velocity was the back location (Fig. 4b). The right side location had the weakest agreement for the HIC$_{15}$ (Fig. 4c). In general, measurements by the raw GFT overestimated measurements made by the HIII for the peak linear acceleration, and HIC$_{15}$ indicated by a large number of the observations above zero along the *y*-axis of the Bland–Altman plots. The exception was the peak rotational velocity, which the raw GFT underestimated compared to the HIII. The corresponding measurement agreement between the HIII and the corrected GFT were improved for all impact parameters. Mean differences between the HIII and the corrected GFT were closer to zero and the 95% limits of agreement were narrower than the raw GFT. The following sections will discuss the coefficients of determination and accuracy (MAPE) of the raw GFT and corrected GFT compared to the HIII for each impact parameter.

Peak Linear Acceleration

There was a strong association, $r^2 = 0.82$, between the peak linear accelerations measured by the raw GFT compared to the HIII, across all of the impact trials ($n = 123$; Fig. 5a). On average, the raw GFT over-predicted the peak linear acceleration measured at the CM of the HIII; the MAPE $\pm$ SD was 49 $\pm$ 21% (Table 1). However, the association improved when the peak linear acceleration of the impacts were calculated with the correction algorithm ($r^2 = 0.97$; MAPE = 4 $\pm$ 4%). The strength of the associations for the raw GFT measurements varied between the individual impact locations. For example, the associations for impacts to the back, facemask, left front boss, left side, right front boss, and right side were all very strong ($r^2 > 0.97$), and impacts to front location had a slightly weaker coefficient of determination ($r^2 = 0.92$; Table 2). Corrected peak linear accelerations from impacts to each impact site better predicted

the peak linear acceleration at the CM of the HIII than the raw GFT; the MAPE $\pm$ SD ranged from 2 $\pm$ 1% for the right side location to 8 $\pm$ 4% for the left front boss location (Table 1).

Rotational Velocity

The association was very strong, $r^2 = 0.94$, between the peak rotational velocity measured by the raw GFT compared to the HIII for all impact trials, (Fig. 5b). In addition, the raw GFT closely predicted the peak rotational velocity at the CM of the HIII (MAPE = 9 $\pm$ 6%; Table 1). Applying the correction algorithm increased both the overall association, $r^2 = 0.96$, and the overall accuracy of the prediction (MAPE = 6 $\pm$ 6%). The corrected GFT measurements were more accurate at measuring the peak rotational velocity at the CM of the HIII than the raw GFT for the back, left front boss, left side, right front boss and right side locations (Tables 1 and 2). Although there were very strong associations ($r^2 = 0.94$ and 0.96), the peak rotational velocities determined by the raw GFT and the corrected GFT did not accurately predict the peak rotational velocity at the CM of the HIII for impacts to the front and left front boss locations (Table 1); these impact locations had MAPE greater than 10%. With one exception, the coefficients of determination for the peak rotational velocities at each impact location either remained the same or increased by using the corrected GFT. In contrast, the right front boss location decreased from 1.00 to 0.99 (Table 2).

HIC$_{15}$

There was a strong association between the HIC$_{15}$ determined from the raw GFT compared to the HIII across all trials ($r^2 = 0.70$; Fig. 5c). However, the raw GFT on average over predicted the HIC$_{15}$ at the CM

TABLE 2. Coefficients of determination (r^2) for the linear regression analyses of the peak linear acceleration, peak rotational velocity, and HIC$_{15}$ between the HIII, raw GFT (rGFT) and corrected GFT (cGFT).

Impact site	Peak linear acceleration		Peak rotational velocity		HIC$_{15}$	
	rGFT	cGFT	rGFT	cGFT	rGFT	cGFT
Back	0.98	0.99	0.96	0.97	0.96	0.97
Facemask	0.94	0.98	0.94	0.96	0.97	0.97
Front	0.81	0.92	0.95	0.95	0.98	0.98
Left front boss	0.98	0.99	0.94	0.96	0.99	0.99
Left side	0.92	0.99	1.00	1.00	1.00	1.00
Right front boss	0.92	0.98	1.00	0.99	0.98	0.98
Right side	0.99	1.00	1.00	1.00	1.00	1.00
All	0.82	0.97	0.94	0.96	0.70	0.98

In general, the correction algorithm improved the coefficient of determinations for the peak linear acceleration across all impact locations.

TABLE 3. Mean absolute percent error (± SD) and coefficients of determination (r^2) for the linear regression analyses of the peak rotational acceleration calculated by the algorithm compared to the peak rotational acceleration from the HIII.

Impact location	Mean percent absolute error (±standard deviation)	Coefficient of detexrmination (r^2)
Back	3 (±2)	0.99
Facemask	15 (±8)	0.82
Front	17 (±16)	0.95
Left front boss	13 (±7)	0.88
Left side	3 (±2)	0.98
Right front boss	9 (±7)	0.97
Right side	3 (±2)	0.99
All	9 (±9)	0.94

The algorithm accurately calculated the peak rotational acceleration for impacts to the back, left side, right front boss, and right side locations.

of the HIII (MAPE = 108 ± 58%; Table 1). The correction algorithm increased the accuracy of the prediction ($r^2 = 0.98$; MAPE = 14 ± 14%). The coefficients of determination were consistently very strong between the HIC$_{15}$ scores at individual impact locations for the raw GFT, $r^2 = 0.96$–0.98. The relationships were also strong for the corrected GFT data (all $r^2 > 0.97$; MAPE = 3 ± 2% to 24 ± 12%; Tables 1 and 2).

Peak Rotational Acceleration Calculated by the Algorithm

The peak rotational acceleration determined by the algorithm had a strong association with the HIII across all trials ($r^2 = 0.94$; MAPE = 9 ± 9%; Table 3). The strength of the associations for the peak rotational accelerations measured by the HIII compared to the peak rotational acceleration calculated from the algorithm was strong for impacts to the back, front, left side, right front boss, and right side locations

($r^2 > 0.95$). Additionally, these impact locations had the least error compared to the HIII (MAPE < 9 ± 7%); the exception was the front location (MAPE = 17 ± 16%; Table 3). The peak rotational acceleration from impacts to the facemask and left boss locations had weaker correlations ($r^2 = 0.82$ and 0.88) and MAPE's greater than 10% (Table 3).

DISCUSSION

The purpose of this study was to evaluate the performance of a wireless accelerometer and gyroscope based device, the gForce Tracker, coupled to the inside of a football helmet, to measure specific head impact parameters compared to measurements from a reference accelerometer package placed at the CM of a HIII anthropometric test dummy headform during controlled laboratory impacts. Linear regression analyses showed strong associations between measurements made from the HIII and raw GFT for the peak linear accelerations, peak rotational velocities, and HIC$_{15}$. The coefficients of determination were improved, and the mean absolute percent error decreased, using correction algorithms based on biases and gain coefficients that varied for each of the impact locations. The algorithm also calculated the peak rotational acceleration of impacts from the rotational velocity from the GFT, which was also strongly associated with the peak rotational acceleration from the HIII.

Peak linear acceleration and rotational acceleration are common biomechanical measures for evaluating the probability of sustaining a concussion.[22] Therefore, it is important for devices to accurately measure these impact parameters at the CM of a person's head when receiving impacts. Results from this study showed that the peak linear accelerations measured by the raw GFT were strongly correlated ($r^2 > 0.82$) to measurements at the CM of a HIII. Like other studies,[1] the strength

of these correlations depended on the impact location on the helmet. However, the peak linear acceleration measured by the raw GFT was up to 75% different than the peak linear acceleration measured at the CM of the HIII (for the right side impact location). The difference in peak linear acceleration between the raw GFT and the HIII in the current study are consistent with results from a previous evaluation of the GFT in hockey helmets.[1] In that study, power fit regression analysis showed a strong relationship between the raw outputs from the GFT used in hockey helmets and the HIII ($r^2 = 0.71$). Similarly, that study showed that there were differences between the raw peak linear accelerations from the GFT and the HIII (MAPE = 100–150%), and the relationships improved after stratifying by impact location ($r^2 = 0.91$–0.96).[1] The authors of that study identified three reasons for these differences: the data had not been transformed from the helmet shell to the CM of the head, the energy absorbed by the helmet during the impact had not been accounted for, and there was some amount of sensor error. Overall the current study shows that the raw GFT output overestimated the peak linear accelerations; on average they were overestimated by 47% (slope of the regression line was 1.47). However, this interpretation is limited given the relatively large amount of random error (MAPE = 49%). The correction algorithm described in the current study addressed the systematic bias and reduced the random error of the raw GFT measuring the peak linear acceleration of head impacts.

The GFT device is equipped with a tri-axial gyroscope so that it measures the rotational velocity of the head from impacts. Although it is not yet a common measure in head impact biomechanics, research has indicated that the magnitude and direction of the rotational velocity and acceleration of the head from an impact can influence mechanisms of injury to the brain.[25,29] As the head/skull begins to rotate, brain tissue will tend to keep its original position and shape with respect to the initial inertial frame. This can create relative brain displacement and deformation in the form of strain.[27] The magnitude of strain and structural damage to the brain can be attributed to the magnitude of the rotational velocity and also the direction of the impact causing the head to rotate.[29] One strength of the GFT is its ability to measure the rotational velocity of impacts. Both the raw GFT and the corrected GFT had an overall strong association to the HIII (slope = 0.94, $r^2 = 0.94$, and MAPE = 9% for the raw GFT and slope = 0.96, $r^2 = 0.96$, and MAPE = 6% for the corrected GFT) for the peak rotational velocity. Our findings with the football helmet are similar to the raw and corrected GFT peak rotational velocities reported in a study on hockey

helmets ($r^2 = 0.83$–0.91, and MAPE = 9–17% for the raw GFT and MAPE = 11–14% for the corrected GFT).[1] Additionally, our findings with the raw and corrected GFT compare favorably to an instrumented mouth guard (slope = 1.00 and $r^2 = 0.98$).[4] Recent injury severity metrics now include the contributions of rotational velocity and acceleration, direction of impact, and impact duration to infer the amount of brain injury.[29] Accordingly devices like the GFT may provide unique and important information.[29]

Like previous studies, a correction algorithm was able to better predict head impact parameters at the CM of the head compared to raw sensor output.[1] This correction algorithm functionally addresses the reasons for the differences in the measurements between the raw GFT and the CM of the head,[1] such as the attenuation due to the helmet padding. In the current study, using the correction algorithm on the raw GFT data led to more accurate predictions (smaller MAPE and r^2 closer to 1.0) for the peak linear acceleration, peak rotational velocity, at the CM of the head, and HIC_{15} parameters. The overall accuracy of the corrected GFT to predict peak linear acceleration at the CM of the head (slope = 0.98 and $r^2 = 0.97$) is comparable to previous validation work with an instrumented mouth guard (slope = 1.01 and $r^2 = 0.96$).[4] The corrected GFT's overall accuracy to predict peak linear acceleration also compared well with previous validation work performed on the standard HIT system, (slope = 1.01 and $r^2 = 0.90$, and the enhanced HIT system designed with additional accelerometers (power regression $r^2 = 0.88$).[2,21] These favorable comparisons to the heavily used standard HIT system research tool provide confidence that the corrected GFT adequately predicts peak linear accelerations at the CM of the head. Additionally, the peak rotational accelerations from the algorithm were strongly associated with measures from the HIII ($r^2 = 0.94$). This compared well to previous evaluations on the instrumented mouth guard ($r^2 = 0.89$) and is superior to the standard HIT system ($r^2 = 0.53$).[2,4] Thus, implementing this algorithm addressed a limitation in the GFT's outputs and resulted in favorable comparisons to other head impact kinematic measuring systems.

There are limitations to the current study. Only one style of helmet, a medium Riddell Revolution Speed helmet, was used for the evaluation testing and the correction algorithm. Different styles of helmets would have different responses in absorbing and dissipating energy from impacts, as shown in hockey helmets.[1] Therefore, separate correction algorithms would need to be developed for different styles of helmets. Additionally, only one GFT mounting location was used in the evaluation testing and development of the correction algorithm. The output of the GFT depends on the

mounting location on the helmet.[1] Consequently, the correction algorithm used in the current study was developed for a GFT mounting location at the top of the Riddell Revolution Speed helmet just left of the crown air bladder. Pilot testing using NOCSAE drop tower methods (velocity of 5.46 m/s and impacts over the left crown) revealed that the GFT sensor did not contact the headform during these worst case scenario tests. This testing also revealed that there were no systematic difference in the resultant peak acceleration measured with the HIII headform for the tests with the GFT mounted in the helmet compared to those without the GFT. However, the architecture of the specific helmet liners will dictate the available mounting sites. Therefore, future work with the GFT device should develop appropriate correction algorithms to allow for multiple mounting locations of the GFT to sports helmets. In addition, all of the laboratory evaluation testing used a HIII headform. Some researchers have identified that it does not have the appropriate nape of the neck geometry for fitting football helmets,[6] and accordingly this may have influenced our findings. Lastly, there was only one testing session with 123 impacts. Additional testing sessions with additional impacts would help to better inform the correction algorithm developed from the current study.

CONCLUSIONS

On average the raw GFT data provided overestimated measures at the CM of the HIII (peak linear accelerations were overestimated on average by 47), but there was a relatively large amount of random error. In contrast, the raw GFT peak rotational velocities of impacts had an overall error of less than 10%. The corrected GFT data accurately predicted the peak linear acceleration, peak rotational velocity, and HIC_{15} compared to measurements at the CM from the HIII and enabled calculation of accurate measures of the peak rotational acceleration. The accuracy of the corrected GFT output was comparable to other devices including an instrumented mouth guard device and the standard HIT system. With injury metrics shifting towards incorporating measures of rotational velocity, and rotational acceleration, the GFT is well suited for future field studies that measure head impact kinematics to athletes.

ELECTRONIC SUPPLEMENTARY MATERIAL

The online version of this article (doi:10.1007/s10439-015-1391-7) contains supplementary material, which is available to authorized users.

REFERENCES

[1]Allison M. A., Y. S. Kang, M. R. Maltese, J. H. T. Bolte, and K. B. Arbogast. Measurement of hybrid III head impact kinematics using an accelerometer and gyroscope system in ice hockey helmets. *Ann. Biomed. Eng.*, 2014.

[2]Beckwith, J. G., R. M. Greenwald, and J. J. Chu. Measuring head kinematics in football: correlation between the head impact telemetry system and hybrid III headform. *Ann. Biomed. Eng.* 40:237–248, 2012.

[3]Bland, J. M., and D. G. Altman. Measuring agreement in method comparison studies. *Stat. Methods Med. Res.* 8:135–160, 1999.

[4]Camarillo, D. B., P. B. Shull, J. Mattson, R. Shultz, and D. Garza. An instrumented mouthguard for measuring linear and angular head impact kinematics in American football. *Ann. Biomed. Eng.* 41:1939–1949, 2013.

[5]Cichos D., D. de Vogel, M. Otto, O. Schaar, and S. Zölsch. Crash analysis criteria description. In: Workgroup Data Processing Vehicle Safety, 2006.

[6]Cobb B. R., A. MacAlister, T. J. Young, A. R. Kemper, S. Rowson, and S. M. Duma. Quantitative comparison of hybrid III and National Operating Committee on Standards for Athletic Equipment headform shape characteristics and implications on football helmet fit. *Proc. Inst. Mech. Eng. Part P* 1754337114548245, 2014.

[7]DiMasi F. Transformation of nine-accelerometer-package (nap) data for replicating headpart kinematics and dynamic loading. Technical Report, 1995.

[8]Gurdjian, E. S., H. R. Lissner, F. G. Evans, L. M. Patrick, and W. G. Hardy. Intracranial pressure and acceleration accompanying head impacts in human cadavers. *Surg. Gynecol. Obstet.* 113:185–190, 1961.

[9]Guskiewicz, K. M., S. W. Marshall, J. Bailes, M. McCrea, R. C. Cantu, C. Randolph, and B. D. Jordan. Association between recurrent concussion and late-life cognitive impairment in retired professional football players. *Neurosurgery* 57:719–726, 2005.

[10]Guskiewicz, K. M., S. W. Marshall, J. Bailes, M. McCrea, H. P. Harding, Jr, A. Matthews, J. R. Mihalik, and R. C. Cantu. Recurrent concussion and risk of depression in retired professional football players. *Med. Sci. Sports Exerc.* 39:903–909, 2007.

[11]Hanlon, E., and C. Bir. Validation of a wireless head acceleration measurement system for use in soccer play. *J. Appl. Biomech.* 26:424–431, 2010.

[12]Langlois, J. A., W. Rutland-Brown, and M. M. Wald. The epidemiology and impact of traumatic brain injury: a brief overview. *J Head Trauma Rehabil* 21:375–378, 2006.

[13]Manoogian, S., D. McNeely, M. Goforth, G. Brolinson, and S. Duma. Head acceleration is less than 10 percent of helmet acceleration during a football impact. *Biomed. Sci. Instrum.* 42:383–388, 2006.

[14]Marar, M., N. M. McIlvain, S. K. Fields, and R. D. Comstock. Epidemiology of concussions among United States high school athletes in 20 sports. *Am. J. Sports Med.* 40:747–755, 2012.

[15]McAllister, T. W., J. C. Ford, L. A. Flashman, A. Maerlender, R. M. Greenwald, J. G. Beckwith, R. P. Bolander, T. D. Tosteson, J. H. Turco, R. Raman, and S. Jain. Effect of head impacts on diffusivity measures in a cohort of collegiate contact sport athletes. *Neurology* 82:63–69, 2014.

[16]McCrea, M., T. Hammeke, G. Olsen, P. Leo, and K. Guskiewicz. Unreported concussion in high school football players: implications for prevention. *Clin. J. Sport Med.* 14:13–17, 2004.

[17]Mihalik, J. P., K. M. Guskiewicz, S. W. Marshall, J. T. Blackburn, R. C. Cantu, and R. M. Greenwald. Head impact biomechanics in youth hockey: comparisons across playing position, event types, and impact locations. *Ann. Biomed. Eng.* 40:141–149, 2012.

[18]National Committee on Standards for Athletic E. Nocsae standard linear impactor test method and equipment used in evaluating the performance characteristics of protective headgear and faceguards. Document #: 1–6, 2006.

[19]Newman, J. A., M. C. Beusenberg, N. Shewchenko, C. Withnall, and E. Fournier. Verification of biomechanical methods employed in a comprehensive study of mild traumatic brain injury and the effectiveness of American football helmets. *J. Biomech.* 38:1469–1481, 2005.

[20]Pellman E. J., D. C. Viano, A. M. Tucker, I. R. Casson, and N. F. L. Committee on Mild Traumatic Brain Injury. Concussion in professional football: location and direction of helmet impacts-Part 2. *Neurosurgery* 53: 1328–1340; discussion 1340–1321, 2003.

[21]Rowson, S., J. G. Beckwith, J. J. Chu, D. S. Leonard, R. M. Greenwald, and S. M. Duma. A six degree of freedom head acceleration measurement device for use in football. *J Appl. Biomech.* 27:8–14, 2011.

[22]Rowson, S., and S. M. Duma. Brain injury prediction: assessing the combined probability of concussion using linear and rotational head acceleration. *Ann. Biomed. Eng.* 41:873–882, 2013.

[23]Rowson, S., S. M. Duma, R. M. Greenwald, J. G. Beckwith, J. J. Chu, K. M. Guskiewicz, J. P. Mihalik, J. J. Crisco, B. J. Wilcox, T. W. McAllister, A. C. Maerlender, S. P. Broglio, B. Schnebel, S. Anderson, and P. G. Brolinson. Can helmet design reduce the risk of concussion in football? *J. Neurosurg.* 120:919–922, 2014.

[24]Signoretti, S., G. Lazzarino, B. Tavazzi, and R. Vagnozzi. The pathophysiology of concussion. *PMR* 3:S359–S368, 2011.

[25]Sullivan, S., S. H. Friess, J. Ralston, C. Smith, K. J. Propert, P. E. Rapp, and S. S. Margulies. Behavioral deficits and axonal injury persistence after rotational head injury are direction dependent. *J. Neurotrauma* 30:538–545, 2013.

[26]Takhounts, E. G., S. A. Ridella, V. Hasija, R. E. Tannous, J. Q. Campbell, D. Malone, K. Danelson, J. Stitzel, S. Rowson, and S. Duma. Investigation of traumatic brain injuries using the next generation of simulated injury monitor (SIMon) finite element head model. *Stapp Car Crash J.* 52(52):1–31, 2008.

[27]Unterharnscheidt, F., and L. S. Higgins. Traumatic lesions of brain and spinal cord due to nondeforming angular acceleration of the head. *Tex. Rep. Biol. Med.* 27:127–166, 1969.

[28]Versace, J. A Review of the Severity Index. Warrendale: SAE, pp. 771–796, 1971.

[29]Weaver, A. A., K. A. Danelson, and J. D. Stitzel. Modeling brain injury response for rotational velocities of varying directions and magnitudes. *Ann. Biomed. Eng.* 40:2005–2018, 2012.

[30]Society of Automotive Engineers (SAE). Instrumentation for Impact Test Part 1: Electronic Instrumentation, SAE J211/1. SAE, 2007.